Unimolecular Dissociation of HOCl Near Threshold: Quantum State and Time-Resolved Studies

Rhett James Barnes, Gregory Dutton, and Amitabha Sinha*

Department of Chemistry and Biochemistry, University of California—San Diego, 9500 Gilman Drive, La Jolla, California 92093-0314

Received: August 14, 1997; In Final Form: September 25, 1997[⊗]

The unimolecular dissociation of HOCl has been examined by accessing several rotational resonances of the $6\nu_{OH}$ vibrational level using overtone−overtone double resonance. An examination of the energetic thresholds for opening various OH fragment rotational states allows us to determine the dissociation energy for the Cl−O bond to be $D_0 = 19\,288.8 \pm 0.6$ cm^{-1} as well as confirm the absence of any appreciable barrier (≤ 2 cm^{-1}) along the reaction coordinate. Time-resolved measurements of the unimolecular dissociation rates arising from excitation to selected $|J,K_a\rangle$ quantum states of the $6\nu_{OH}$ vibrational level are found to be substantially slower than that expected on the basis of RRKM theory, and as a function of energy, these rates exhibit recurrent maxima that approximately correlate with the rotational energy level spacings of the OH($^2\Pi_{3/2}$) manifold. The OH fragment product state distributions resulting from near-threshold unimolecular dissociation are found to be hotter than those predicted by phase space theory.

Introduction

A central assumption of RRKM theory is that energy flow within a vibrationally excited molecule is complete on a time scale much faster than dissociation.[1] State-selected unimolecular dissociation of small polyatomic molecules where vibrational state mixing is restricted, and hence IVR rates are slow, provides a critical test of the limits of statistical behavior. In this paper we present initial results on the *state and time*-resolved unimolecular dissociation of HOCl near its energetic threshold corresponding to excitation of various rotational resonances of the fifth O−H stretching overtone ($6\nu_{OH}$). The low vibrational state density in HOCl combined with the large disparity in the vibrational frequency between the O−H (3600 cm^{-1}) and Cl−O (700 cm^{-1}) stretching coordinates suggests that energy flow within the molecule may be restricted when the system is energized through vibrational overtone excitation. As a result the unimolecular reaction rate for this system can potentially exhibit nonstatistical behavior. In addition, because the dissociation process generates two radical fragments, OH + Cl, the potential energy surface is likely to be barrierless along the reaction coordinate and hence allows an examination of the extent to which the product state distribution behaves statistically. There are many examples of nonstatistical behavior that have been observed in the dissociation dynamics of van der Waals molecules, where the frequency of the van der Waals bond is substantially lower than those of the other bonds in the system.[2] For covalently bonded molecules, however, statistical theories have, in general, done a remarkable job in describing the dissociation dynamics even for molecules as small as NO_2.[3,4] Below we present results of an experiment using overtone−overtone double resonance that measures the unimolecular dissociation rate and product state distribution resulting from excitation of selected $|J,K_a\rangle$ resonances in HOCl and examines the extent to which these findings agree with statistical theories.

Experimental Section

The apparatus and vibrational overtone−overtone double-resonance excitation scheme used in the present experiment are similar to that described in our earlier work on the $7\nu_{OH}$ band of HOCl.[5] Briefly, HOCl molecules at room temperature are first excited to the $2\nu_{OH}$ vibrational state using infrared light from an OPO (∼10 mJ, 0.3 cm^{-1}). The energized molecules are subsequently further excited to selected J,K_a rotational resonances of the $6\nu_{OH}$ vibrational state using a dye laser operating in the region of 830 nm (∼30 mJ, 0.08 cm^{-1}). The OH fragments resulting from the dissociation are probed by laser-induced fluorescence using the frequency-doubled output of a third Nd:Yag pumped dye laser system. Although we do not detect the chlorine atom in these experiments, they are expected to be formed in the $^2P_{3/2}$ spin−orbit state. The excited Cl($^2P_{1/2}$) state lies ∼882 cm^{-1} higher in energy and is not accessible in these near-threshold measurements. We typically operate at a total pressure of ∼20 mTorr and keep the time delay between the two vibrational excitation lasers at ∼ 20 ns. Monitoring a particular quantum state of the OH fragment as the frequency of the dye laser (corresponding to the second step of the double-resonance process) is scanned generates an action spectrum of HOCl revealing the resonances that produce OH fragments in the interrogated quantum state. Varying the time delay between the probe laser and the dye laser initiating the $2\nu_{OH} \rightarrow 6\nu_{OH}$ excitation provides the means for characterizing the dissociation rates. The absolute frequency of both vibrational excitation lasers involved in the double resonance are calibrated relative to H_2O transitions using photoacoustic spectroscopy.[6]

Results and Discussion

The first requirement for implementing the double-resonance scheme involves characterization of the intermediate vibrational state. For HOCl, we have examined the $2\nu_{OH}$ vibrational level using the technique of vibrationally mediated photodissociation.[7] In a separate set of experiments, HOCl molecules at room temperature are first vibrationally excited to the $2\nu_{OH}$ level using infrared light from the OPO and then subsequently photodissociated using UV light at 355 nm from a Nd:Yag laser. Monitoring the yield of a particular quantum state of the OH fragment resulting from photodissociation, as the frequency of the OPO is varied, generates the action spectrum shown in Figure 1a. The spectrum consists of both perpendicular and parallel transitions characteristic of a hybrid band of a near-

[⊗] Abstract published in *Advance ACS Abstracts,* November 1, 1997.

S1089-5639(97)02668-6 CCC: $14.00

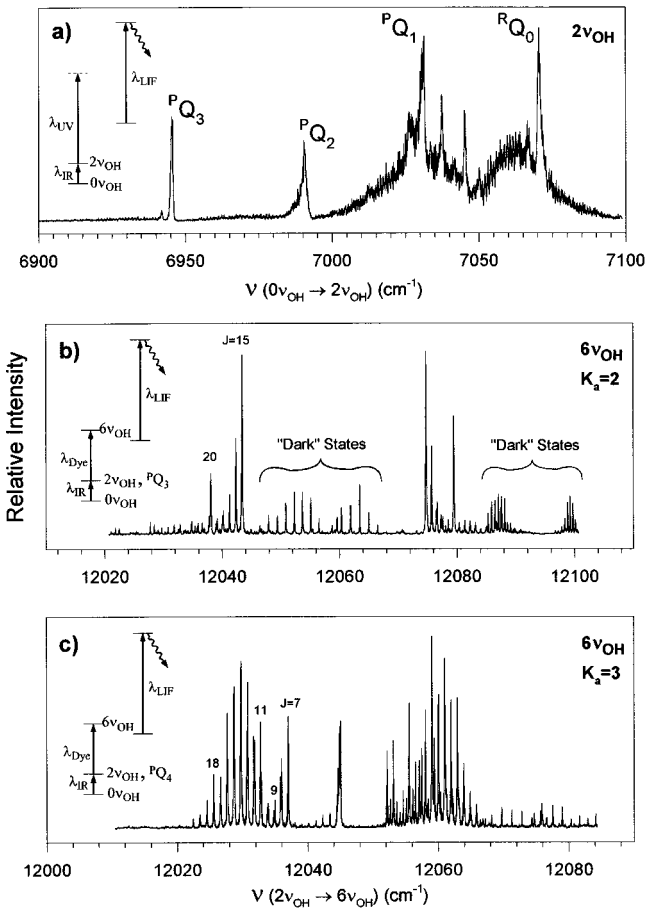

Figure 1. (a) Action spectrum of the HOCl $2\nu_{OH}$ vibrational state obtained by photodissociating HOCl($2\nu_{OH}$) through electronic excitation using 355 nm light while monitoring the yield of OH(v''=2,N=2) fragments as the vibrational excitation laser frequency is scanned. (b) Action spectrum of the $2\nu_{OH} \rightarrow 6\nu_{OH}$ transition with the IR laser frequency set on the $^PQ_3$ stack shown in Figure 1a while probing the OH(v''=0,N=1,$^2\Pi_{3/2}$) state resulting from unimolecular dissociation. The transitions labeled as "dark states" are as yet unidentified vibrational states that appear as a result of intensity borrowing from the bright $6\nu_{OH}$ stretching state. (c) Action spectrum of the $2\nu_{OH} \rightarrow 6\nu_{OH}$ transition with the IR laser parked on the $^PQ_4$ stack while probing the OH(v''=0,N=1,$^2\Pi_{3/2}$) state resulting from unimolecular dissociation.

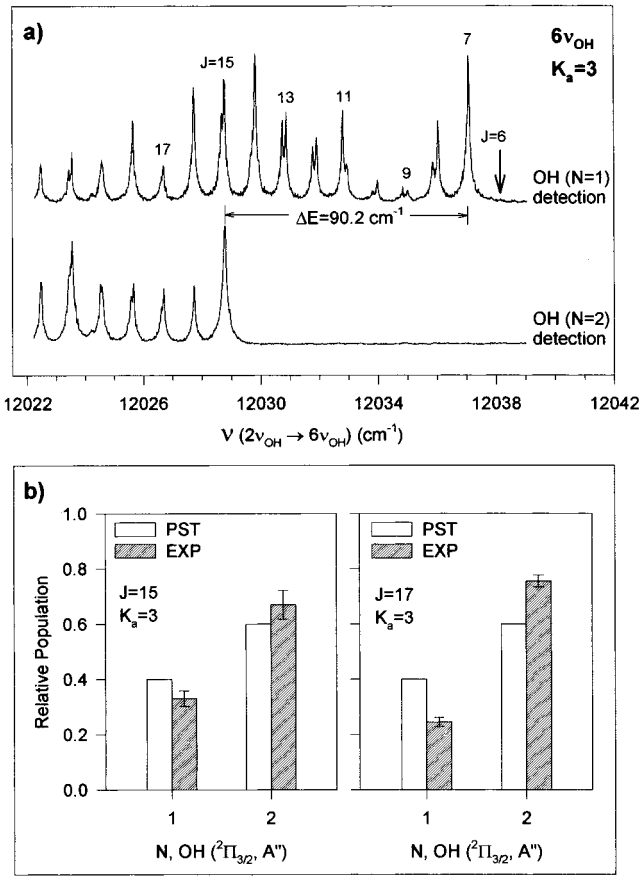

Figure 2. (a) Action spectra for transitions belonging to the $K_a = 3$ stack. The upper trace is obtained by monitoring the OH(v''=0,N=1,$^2\Pi_{3/2}$) product state while the frequency of the $2\nu_{OH} \rightarrow 6\nu_{OH}$ excitation step is scanned. The lower trace is a scan over the same region obtained by monitoring OH(v''=0,N=2,$^2\Pi_{3/2}$). (b) Comparison of measured OH fragment product state distribution with phase space theory resulting from excitation of two nearby resonances. The distribution on the left corresponds to excitation of the $J = 15$, $K_a = 3$ resonance while the one on the right corresponds to the $J = 17$, $K_a = 3$ resonance. The error bars shown reflect the $\pm 2\sigma$ limit. These distributions are independent of the time delay between the state preparation and probe lasers.

prolate symmetric top. The assignments shown are based on the earlier work of Cavazza et al. using high-resolution absorption spectroscopy.[8] Having determined the location of various spectral features belonging to the $2\nu_{OH}$ level, we are able to implement the double-resonance technique to investigate unimolecular reaction.

Figure 1b shows the results of parking the OPO on transitions belonging to the $^PQ_3$ stack of the $2\nu_{OH}$ intermediate vibrational state and then scanning the dye laser corresponding to the $2\nu_{OH} \rightarrow 6\nu_{OH}$ excitation step. Figure 1c shows the analogous data with the OPO parked on the $^PQ_4$ stack of the $2\nu_{OH}$ band. By parking the OPO on various other K_a-stacks of the $2\nu_{OH}$ spectrum shown in Figure 1a and then scanning the dye laser, we can effectively decompose the $2\nu_{OH} \rightarrow 6\nu_{OH}$ excitation spectrum into its K_a components. For both spectra in Figure 1b,c the probe laser monitors population in the lowest rotational level of the OH fragment, the $N = 1$ state of the $^2\Pi_{3/2}$ manifold. As can be seen from comparing the spectrum in Figure 1a with those of Figure 1b,c, the double-resonance approach allows access to rotationally resolved spectra of the $6\nu_{OH}$ vibration even though state selection in the $2\nu_{OH}$ intermediate state is incomplete due to the modest line width of our OPO ($\sim$0.3 cm^{-1}). The rotational assignment shown in Figure 1b,c has been verified by checking known intermediate state combination differences as discussed in our $7\nu_{OH}$ work.[5] As Figure 1b shows, in addition to detecting transitions belonging to the zeroth-order $6\nu_{OH}$ state, we also observe transitions to yet unassigned "dark" background states in the region. The $6\nu_{OH}$ state, which involves O−H stretching motion, is the "bright" zeroth-order state that carries the oscillator strength in the overtone transition. Coupling of this zeroth-order "bright" state to nearby "dark" states containing excitation in other vibrational degrees of freedom allows us to see the "dark" states through intensity borrowing.

Since the band origin of the $6\nu_{OH}$ vibrational level is below the dissociation threshold, energy constraint limits the rotational states seen in the action spectrum to those having sufficient energy to dissociate. Consequently, by monitoring the energetic threshold where the *lowest* rotational level of the OH fragment just turns on, it is possible to obtain an estimate of the HO−Cl bond dissociation energy. Of course in these double-resonance experiments we are unable to vary the energy of the parent molecule continuously and rely on the "comb" of rotational resonances accessible within each K_a-stack. The upper trace in Figure 2a is an expanded view of the P-branch region of the $K_a = 3$ stack obtained by monitoring the OH(N=1;$^2\Pi_{3/2}$) quantum state as the $2\nu_{OH} \rightarrow 6\nu_{OH}$ excitation is scanned. The position of the first observed HOCl rotational transition in this

action spectrum, the $J = 7$ resonance, provides a limit on the threshold energy for dissociation. Similar threshold data have been collected by monitoring the OH(N=1;$^2\Pi_{3/2}$) state while scanning over transitions belonging to the $K_a = 2$ stack as well. From the known energies of the transitions involved in these "threshold" resonances, the Cl−O bond dissociation energy is estimated to be $D_0 = 19\,288.8 \pm 0.6$ cm^{-1} for the dominant HOCl^{35} isotope.

In addition to determining D_0, we have examined the possibility of a barrier along the reaction coordinate by monitoring the appearance threshold of OH rotational levels lying above the OH(N=1;$^2\Pi_{3/2}$) state. In the absence of a barrier, the difference in threshold energy for opening the lowest energy product state and another product state lying above it is expected to be identical with the corresponding energy level spacing occurring in the isolated fragment. The presence of a barrier, however, is expected to *reduce* this number by an amount dictated by the barrier height. The lower trace in Figure 2a illustrates this approach for the OH(N=2;$^2\Pi_{3/2}$) state. The energy difference between the $N = 1$ and $N = 2$ rotational states in free OH is 83.9 cm^{-1}. Thus the extent to which the measured threshold energy for opening the OH(N=2) state agrees with this value allows us to place stringent limits on the barrier height. The fact that the HOCl resonance corresponding to $J = 14$, $K_a = 3$, which lies 75.4 cm^{-1} above D_0, has not turned on (see lower trace of Figure 2a) and the first observed resonance to turn on when OH(N=2) is monitored is the $J = 15$, $K_a = 3$ state implies the absence of any barrier that is higher than 8.5 cm^{-1}. Our inability to get a better bound on this number using resonances in the $K_a = 3$ stack results from our inability to vary the available energy continuously. However, doing the same measurement, of monitoring the relative thresholds for producing OH(N=1) vs OH(N=2), using resonances in the $K_a = 2$ stack allows us to get a slightly better estimate and conclude that there are no barriers along the reaction coordinate to within an uncertainty of 1.6 cm^{-1}.

We note that apart from barriers arising from electronic interactions there may also be contributions from centrifugal barriers. We have examined this possibility and believe that their effects are small for the range of angular momentum states discussed above (i.e. $J = 7-15$). That this is so can be seen by treating the dissociation of HOCl as a two-body problem and noting that for a given angular momentum state, J, the magnitude of the associated centrifugal barrier is given by:

$$V_{max} = (J(J+1)h^2/4\pi^2\mu)^{3/2}(1/3(6C_6)^{1/2})$$

In the above expression μ is the reduced mass of the OH and Cl fragments, h is Planck's constant, and C_6 is the coefficient describing the attractive part of the long range interaction arising from dipole-induced dipole and dispersion forces. Using a value of $C_6 = 1.0 \times 10^{-77}$ J m^6, which is a lower limit value that we obtain from the results of the phase space calculations discussed below, we find that for the $J = 7$ state the centrifugal barrier is less than 0.41 cm^{-1} and this barrier rises to at most 3.6 cm^{-1} when considering the $J = 15$ state. Thus, effects due to centrifugal barriers are rather small for the states considered above.

Previous studies of unimolecular reactions occurring on a barrierless potential have found that phase space theory[9] is able to accurately describe the product state distribution for excitation energies near the dissociation threshold.[10] We have begun to examine these ideas for HOCl by measuring OH fragment rotational state distributions resulting from excitation of different rotational resonances. The bar graph on the left side of Figure 2b shows the product state distribution resulting from excitation of the $J = 15$, $K_a = 3$ resonance (shown in lower frame of Figure 2a), which is the lowest energy resonance that can produce the OH(N=2,$^2\Pi_{3/2}$) quantum state and lies at an energy of 90.2 cm^{-1} above D_0. In contrast the distribution shown on the right of Figure 2b arises from excitation of the $J = 17$, $K_a = 3$ resonance lying 122.8 cm^{-1} above D_0. Comparison of the measured distributions with those predicted by phase space theory reveals (see Figure 2b) that the measured distributions are hotter than predicted with the deviation being larger for the $J = 17$, $K_a = 3$ resonance. It is worth pointing out that the value of the C_6 coefficient used in the phase space calculations, $C_6 = 1.0 \times 10^{-77}$ J m^6, was determined empirically by requiring the results of the simulation to match the experimental distribution as closely as possible. We find that the value of C_6 coefficient that gives the best match with experiment is slightly larger than that estimated from using the known dipole moment, polarizabilities, and ionization potentials of the fragments. Using the calculated value of the C_6 coefficient, $C_6 = 5.5 \times 10^{-78}$ J m^6, in a phase space calculation generates rotational state distributions that are substantially colder than what is experimentaly observed. Using values of the C_6 coefficient larger than $C_6 = 1.0 \times 10^{-77}$ J m^6 did not change the results of the calculations. Thus it appears that the calculated value of the C_6 coefficient underestimates the long range attractive part of the potential in HOCl; a similar trend has been also been noted in NO_2 and ketene.[3c,10a] In addition, we have examined whether the measured distributions shown in Figure 2b depend on the time delay between the state preparation and probe lasers and find them to be independent of this parameter.

The dissociation rate of HOCl from the $6\nu_{OH}$ vibrational state is sufficiently slow as to allow a direct measurement of the time evolution of the OH fragments using our nanosecond laser system. Thus, we are able to determine the unimolecular dissociation rates in this molecule as a function of the $|J,K_a\rangle$ quantum numbers. The various panels in Figure 3 illustrate how these rates vary with the angular momentum quantum number, J, within each indicated K_a-stack for energies ranging from just below the dissociation threshold to ∼201 cm^{-1} above this limit. The first thing one notices is that the measured rates are substantially slower than that expected on the basis of RRKM theory, which expresses the energy dependence of the rate as $k(E) = N^{\#}(E - E_0)/h\rho(E)$.[1] Application of this equation to HOCl at threshold where $N^{\#} = 1$ and the density of vibrational states is $\rho \approx 0.15$ states/cm^{-1} gives $k_{RRKM} \approx 2 \times 10^{11}$/s. By contrast the measured rate for the $J = 7$, $K_a = 3$ resonance, which corresponds to the state closest to the threshold, is $k \approx 5 \times 10^7$/s. The magnitude of the measured rate suggests that energy flow out of the OH stretching coordinate is extremely slow in HOCl.

Previous unimolecular dissociation studies on singlet CH_2-CO[11] and NO_2,[3a,b] where RRKM theory has worked well, have observed a stepwise increase in the reaction rate as a function of excitation energy and have interpreted these "steps" as arising from the sequential passing of energetic threshold for opening vibrational levels of the transition state. In HOCl we find that, for excitation energies ranging up to ∼100 cm^{-1} above the dissociation threshold, there is a peaking of the reaction rates as the threshold for opening each OH($^2\Pi_{3/2}$) product state is crossed. However, unlike the situation in CH_2CO and NO_2, we do not observe a leveling of the rates for excitation energies lying between these thresholds. For example, in the $K_a = 2$ stack (see Figure 3a), we see that the rate starts out at zero for energies below the threshold for dissociation, reaches a peak value just as the threshold for generating OH(N=1,$^2\Pi_{3/2}$) is crossed at $J = 15$, then starts to monotonically decrease until J

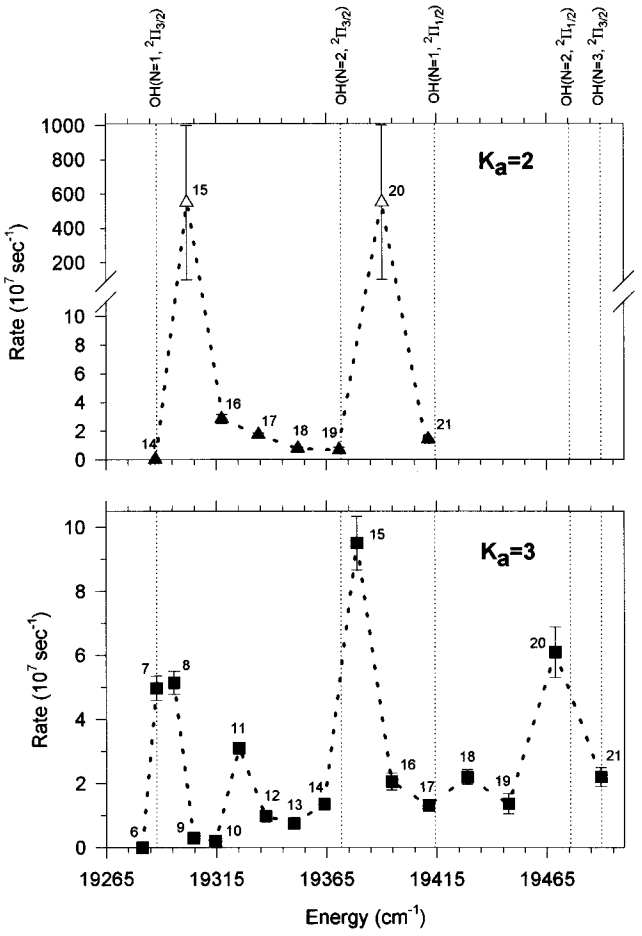

Figure 3. Variation in unimolecular dissociation rates of HOCl($6\nu_{OH}$) as a function of energy for various angular momentum states, J, in the (a) $K_a = 2$ and (b) $K_a = 3$ manifolds. Although not shown, the rates for the ($J = 22$, $K_a = 3$) and ($J = 23$, $K_a = 3$) resonances are substantially slower than that for ($J = 20$, $K_a = 3$). The rates were determined by monitoring the time evolution of the OH(v''=0,N=1,$^2\Pi_{3/2}$) state and fitting the appearance curve to a single exponential.

$= 20$ where it rises again as the threshold for making the OH(N=2,$^2\Pi_{3/2}$) rotational state is crossed. In fact the dissociation rates for $J = 15$, $K_a = 2$, and $J = 20$, $K_a = 2$ are so large that we are unable to measure them directly with our nanosecond laser system. The error bars shown in Figure 3a for the rates of these two resonances indicate the limits placed on their value based on line width measurements ($\Delta\nu \approx 0.08$ cm^{-1}) combined with our inability to observe time evolution of the product faster than the 5−10 ns level. Similar trends in the rates are again observed for the J levels belonging to the $K_a = 3$ stack (see Figure 3b). Their rates are also observed to peak in the first ~100 cm^{-1} as the energetic thresholds for opening OH(N=1, $^2\Pi_{3/2}$) and OH(N=2,$^2\Pi_{3/2}$) product rotational states are passed; although at energies between the amount required to open these two product states substantially more fluctuation is observed in the rates for resonances in the $K_a = 3$ stack than for those in the $K_a = 2$ manifold (compare Figure 3a with Figure 3b). As the density of vibrational states in HOCl is low, the observed fluctuations most likely either reflect variation in state mixing as some rotational levels of the "bright" $6\nu_{OH}$ stretching state happen to be more efficiently coupled to nearby "dark" background states, thus enhancing their coupling to the dissociative continuum, or the fluctuation may just reflect random variation in the coupling matrix elements between the transition state and final product states.[12] Apparently, as the excitation energy is increased, the spacings between the prominent maxima no longer exactly match the rotational level spacing of the OH($^2\Pi_{3/2}$) manifold, and the next major peak that is observed occurs at the ($J = 20$, $K_a = 3$) resonance, whose energy is slightly below that required to open the OH(N=3,$^2\Pi_{3/2}$) state. Although not shown in Figure 3, we have gone to even higher excitation energies using resonances of the $K_a = 5$ stack and find that the next peak in reaction rate occurs at an energy, $E = 19\,640.58$ cm^{-1}, corresponding to the ($J = 16$, $K_a = 5$) resonance, which is just below the threshold for opening the OH(N=4,$^2\Pi_{3/2}$) state. One possible explanation for the observed trends is that the peaks in the rates occur for those quantum states which are sufficiently strongly coupled to facilitate conversion of energy stored as rotation about the a-axis into vibrational energy for motion along the reaction coordinate. Why the location of the various maxima should roughly correspond to the levels of the $^2\Pi_{3/2}$ spin-orbit manifold is an interesting question which we hope to address in future work. We are currently measuring dissociation rates at higher excitation energies in order to test these ideas in greater detail.

Acknowledgment. We thank the National Science Foundation for support of this work. In addition we thank the Hellman Foundation of UC San Diego for partial support of this research.

References and Notes

(1) (a) Gilbert, R. G.; Smith, S. C. *Theory of Unimolecular and Recombination Reactions*; Blackwell Scientific: Oxford, 1990. (b) Baer, T.; Hase, W. L. *Unimolecular Reaction Dynamics*; Oxford University Press: Oxford, 1996.

(2) (a) Huang, Z. S.; Jucks, K. W.; Miller, R. E. *J. Chem. Phys.* **1986**, *85*, 3338. (b) Huang, Z. S.; Miller, R. E. *J. Chem. Phys.* **1989**, *90*, 1478. (c) Kerstel, E. R. Th.; Scoles, G.; Yang, X. *J. Chem. Phys.* **1993**, *99*, 876.

(3) (a) Miyawaki, J.; Yamanouchi, K.; Tsuchiya, S. *J. Chem. Phys.* **1993**, *99*, 254. (b) Ionov, S. I.; Brucker, G. A.; Jasques, C.; Chen, Y.; Wittig, C. *J. Chem. Phys.* **1993**, *99*, 3420. (c) Hunter, M.; Reid, S. A.; Robie, D. C.; Reisler, H. *J. Chem. Phys.* **1993**, *99*, 1093. (d) Reid, S. A.; Reisler, H. *J. Phys. Chem.* **1996**, *100*, 474. (e) Reid, S. A.; Reisler, H. *Annu. Rev. Phys. Chem.* **1996**, *47*, 495.

(4) Houston, P. Conference on the Dynamics of Molecular Collisions, Gull Lake, 1997; Abstract.

(5) Barnes, R. J.; Sinha, A. *J. Chem. Phys.* **1997**, *107*, 3730.

(6) (a) Rothman, L. S.; Gamache, R. R;. Goldman, A.; Brown, L. R.; Toth, R. A.; Pickett, H. M.; Poynter, R. L.; Flaud, J.-M.; Camy-Peyret, C.; Barbe, A.; Husson, N.; Rinsland, C. P.; Smith, M. A. H. *Appl. Opt.* **1987**, *26*, 4058. (b) AFGL Hitran Data Base, 1986.

(7) Crim, F. F. *Annu. Rev. Phys. Chem.* **1993**, *44*, 397.

(8) Cavazza, F.; Di Lonardo, G.; Escribano, R.; Fusina, L.; Gomez, P.C.; Ortigoso, J. *J. Mol. Spectrosc.* **1993**, *159*, 395.

(9) (a) Pechukas, P.; Light, J. C. *J. Chem. Phys.* **1965**, *42*, 3281. (b) Pechukas, P.; Light, J. C.; Rankin, C. *J. Chem. Phys.* **1966**, *44*, 794.

(10) (a) Wade, E. A.; Clauberg, H.; Kim, S. K.; Mellinger, A.; Moore, C. B. *J. Phys. Chem.* **1997**, *101*, 732. (b) Qian, C. X. W.; Noble, M.; Nadler, I.; Reisler, H.; Wittig, C. *J. Chem. Phys.* **1985**, *83*, 5573. (c) Hunter, M.; Reid, S. A.; Robie, D. C.; Reisler, H. *J. Chem. Phys.* **1993**, *99*, 1093.

(11) (a) Lovejoy, E. R.; Kim, S. K.; Moore, C. B. *Science* **1992**, *256*, 1541. (b) Kim, S. K.; Lovejoy, E. R.; Moore, C. B. *J. Chem. Phys.* **1995**, *102*, 3202.

(12) Miller, W. H.; Hernandez, R.; Moore, C. B.; Polik, W. F. *J. Chem. Phys.* **1990**, *93*, 5657.